Brandon J.N. Long, Hans D. Hallen, "Resonance Raman techniques for complex biological systems", Proceedings of SPIE Vol. 11122, 1112222 (2019), doi 10.1117/12.2529642.

Resonance Raman techniques for complex biological systems

Hans D. Hallen[a] and Brandon J.N. Long[a]

[a]Department of Physics, North Carolina State University, 2401 Stinson Dr, Raleigh NC, USA

ABSTRACT

Resonance Raman offers a significant increase in Raman signal levels. We show how this can be used to select a specific molecule within a complex biosystem to study, in our case to determine if hemoglobin survives in ancient fossils. Key to this ability is the fact that the vibration must be on the same molecule as the absorption. Further, we show that the Raman fingerprint, or changes to it, can provide further selectivity or identify changes in that molecule based upon the particular sample. In our case, we find that the iron in the hemoglobin has oxidized into FeOOH, but still attached to both its porphyrin-like heme group and the protein network that gives the hemoglobin absorption. Very narrow Raman resonances are found in molecules with symmetry-forbidden, phonon-allowed absorptions. We show several in biologically relevant materials including that methylated-DNA (m-DNA) can be distinguished from non-methylated (n-DNA) with nano-bowtie- and resonance- enhanced Raman spectra. These effects are retained when plasmon resonances are used to enhance a local region of the sample, but find that the overall signal from a uniformly distributed specimen is not increased significantly by the enhancement of a small region, so is not recommended unless the sample can be concentrated into that region.

Keywords: resonance Raman, plasmon resonance, selectivity, Raman fingerprint, biological imaging, ancient soft tissue, hemoglobin, cytosine

1. INTRODUCTION

The last several decades have seen a drastic increase in molecular studies on living organisms. These data inform every aspect of biology. However, there is a dearth of similar studies on very old fossils, because of the prevailing wisdom that biomolecules will completely degrade before one million years (Ma).[1–4] The discovery of still soft, flexible microstructures consistent with blood vessels, cells and extracellular bone matrix in multiple extinct organisms recovered from multi-million year old sediments[5–12] has led to the reexamination of this central hypothesis of degradation.[10,13,14] Here, we present additional data supporting the endogeneity of these microstructures, preserved via a proposed hemoglobin reaction.

Previous studies on these soft tissue materials have employed multiple high resolution techniques, including immunological assays using specific antibodies;[12,15] various mass spectrometry methods;[12,16] vibrational mode spectroscopy methods, including high resolution, solution-phase proton NMR, electron spin resonance; and surface enhanced Raman spectroscopy. These were used to analyze a well preserved specimen of Tyrannosaurs rex (MOR 555,[17]), supporting the persistence of a hemoglobin-like compound in bulk extracts of cortical bone.

Resonance Raman spectroscopy can simplify analyses of complex materials like fossil bone. Every Raman active molecule has a characteristic Raman spectrum, which can then be compared to Raman spectra from a wide range of literature.[11,18–25] Although Raman spectra can aid in identification of molecular components, its spectral resolution in this case is limited, in part by low sample order[12] typical of biological samples, as compared to crystal samples.[26–29] Resonance Raman overcomes some of these obstacles to obtaining high resolution characterizations of complex samples.[30] By tuning the excitation wavelength to the known absorbance

Further author information: (Send correspondence to H.D.H.)
H.D.H.: E-mail: hallen@ncsu.edu
B.J.N.L.: E-mail: bjnlong@gmail.com

of a molecule, the absorbing molecules Raman spectra greatly increases.[12,16,26–28,31–37] Although the vibrations typically measured with Raman in the few hundreds to few thousands of wavenumbers generally correspond to functional groups, the absorption spectra of a molecule typically involves larger structures acting in concert. This is especially true in hemoglobin, where O_2 binding to the heme moiety causes dramatic shifts in the quaternary structure of the molecule and therefore the absorption.[15] Because only the vibrations associated with that particular absorptive feature are Raman-enhanced,[17] resonance Raman provides double-selectivity in identifying the molecule and the vibrations associated with it.[38] We have produced evidence of resonance phenomena in the intensity of the Raman returns from these samples.[39] Here, we quantify the enhancement and show returns consistent with hemoglobin in these samples. Thus, any alternative explanations must explain both the resonance phenomenon and the Raman signal. This is a type of doubly-selective test.

It is important to note that, for a Raman spectra to be resonance Raman, there must be a feature of the sample that is resonating. Here, we use an absorptive feature of the molecule to drive a resonance in the Raman process. Surface-enanced Raman scattering (SERS) uses plasmonic modes in metallic dots to drive a plasma resonance that increases the excitation strength, hence the Raman signal. If we do not see this enhancement, we cannot claim that we see either plasmon-enhanced Raman, SERS, or resonance Raman. This is the basis of one part of our doubly-selective test, and as such, we must take care to note when this condition is satisfied, and by what, when comparing to other literature. Note also that a resonance Raman spectrum can contain different relative peak heights and multiplets/overtones compared to a non-resonant Raman spectrum.

Previously, it was hypothesized that these vessels were preserved through interactions between heme-derived iron and the endothelial cell membranes that form blood vessel walls in vertebrate organisms.[40] One proposed chemical pathway for vessel preservation involves iron available from hemoglobin catalyzing a redox cycle to crosslink vessel collagen.[40,41] Resonance Raman is a good tool for studying the distribution of hemoglobin in the sample, as it allows us to probe the distinctive bond energies of these molecules. We need to choose exciting wavelengths that both coincide with hemoglobin molecular absorption and do not.[40] Another important goal was to discriminate endogenous heme from other molecules that might be present in the samples.[42] Data from reference samples and from modern analogues will provide a basis for comparison.[43]

2. METHODS

2.1 Sample Preparation

In addition to the samples below, we also took data on whole blood taken from an author, as a reference. We used this to both provide an on-resonance spectral measurement for reference, and calculate the resonance enhancement, as described in section Section 3.1 below.

2.1.1 Ancient Vessels

Our ancient samples were prepared in a laboratory dedicated to analyses of fossil tissues, exclusive of any extant material. Cortical bone fragments from the B. canadensis femur were demineralized in 500 mM ethylenediaminetetraacetic acid (EDTA) pH 8.0 for two weeks. We then isolated and collected the blood vessels from the demineralized bone fragments. We washed blood vessels with E-pure water 10 times to completely remove the EDTA, and then stored them in water to complete preparation for further Raman analysis.

2.1.2 Modern Vesels

Cortical bone fragments from ostrich femur were demineralized in 500 mM EDTA until all mineral was removed. After demineralization, 1 mm thick slices were cut and then washed 10-20 times with e-pure water to remove EDTA before collagenase digestion. Slices were then resuspended in 2 ml of 1mg/ml collagenase A (Roche) in Dulbuccos phosphate buffered saline and allowed to digest overnight at 37°C. The remaining vessels were washed with E-pure water 4 times to remove residual collagenase. To fully simulate ancient preservation, these modern

vessels were then immersed in different environments: deoxygenated Hb in 2 ml micro centrifuge tube under deoxygenated environment, and oxygenated water under same condition as control. These hemoglobin solutions are described below.

We separated 100 ml chicken whole blood-k3EDTA from Lampire bio lab cat#7208808 aliquot to 20 Tubes and washed this blood with 0.9% NaCl isotonic saline. Afterwards, we centrifuged the solution for 15 min at 5000g to remove plasma, serum and WBC. We processed equivalent with 3.75 mM phosphate buffer for 1hr in ice-water bath, centrifuge at 5000g for 15 min, and repeated 3 times. We filtered this solution through glass wool, and then through 0.45um syringe membrane filter. Finally we ultra filtered the solution with 3 kD Amicon ultra centrifugal filter and change buffer to e-pure water. The desalted solution was collected and referred as hemoglobin solution total 8x12 ml. For the deoxygenated sample, the Chicken Hb solution was degassed by ultra-sonic and the surface was purged with carbon dioxide (CO_2) for several hrs. The processing chamber was purged with CO_2 then sealed for deoxygenated environment. The chamber continue purged with carbon dioxide once a day.

2.2 Choice of Excitation Wavelengths for Resonance

2.2.1 Absorption Spectra of Single Chemicals

Generally, the absorptive features that drive resonance Raman are tens of nanometers wide in wavelength, as they are symmetry allowed. This allows us to use fixed wavelength lasers, without fear of missing the resonance. Fig. 1 compares the absorption spectra of hemoglobin and heme, two molecules that we would like to be able to test for. We note a distinguishing feature near 550 nm for the hemoglobin. This feature is different in the oxygenated and deoxygenated state of hemoglobin, due to the molecule shifting from a relaxed (R) state to a tense (T) state.[44] Since this corresponds to a well known shift in the quaternary structure of hemoglobin, this peak is highly correlated to the structure of the whole molecule.

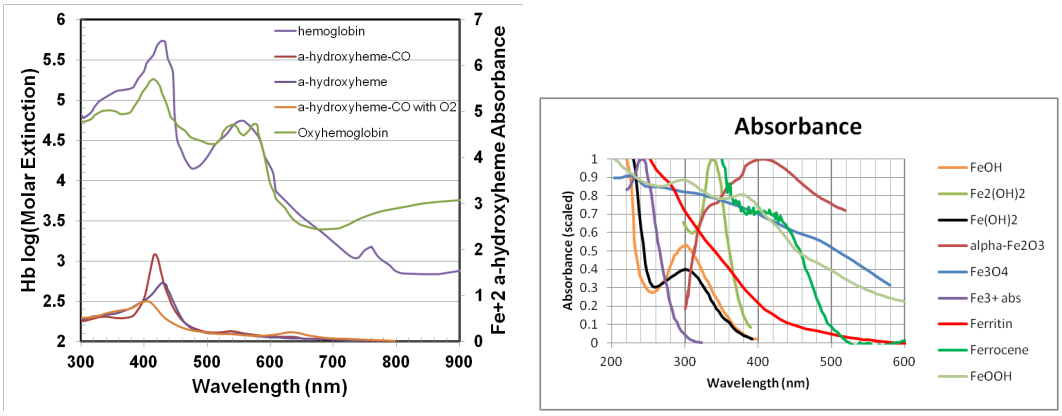

(a) (b)

Figure 1 (a)The normalized (to 300 nm value) absorption spectra of hemoglobin from[45] and heme from[46] are compared to the two laser wavelengths used so that resonance conditions can be evaluated. (b)Absorbance spectra of various minerals and a few organic compounds. FeOOH spectra after;[47] Ferritin spectra after;[48] Ferrocene spectra after;[49] α-Fe_2O_3 spectra after;[50] Fe_3O_4 spectra after;[51] all others after.[52] Note that no chemical is more absorptive near 532 nm than 473 nm, indicating any resonance activity near 532 nm is due to hemoglobin

To satisfy these constraints, we chose two lasers as our exciting wavelengths. One, providing excitation at 532 nm, is just to one side of the absorbing peak in hemoglobin, and thus, will display resonant behavior due to hemoglobin regardless of oxidation state. The other is a 473 nm laser, which is closer to heme's resonant peak, and further from hemoglobin's. Therefore, if we see a resonance at 532 nm excitation but not at 473 nm excitation, it is due to hemoglobin (or its constituent myoglobin). As such, we examine some common iron oxides as well as ferrocene and ferritin. These chemicals have their absorption spectra graphed in Fig. 1.

We note that most of the minerals are not absorbent at wavelengths longer than 400 nm. Of those that are significantly absorbent into the visible spectrum, they are more absorbent near 473 nm than near 532 nm, so the same resonance source applies. As such, our measuring schema will show dramatic resonance behavior near 532 only if the absorptive hemoglobin feature is still intact.

2.2.2 Laser Wavelengths and Fluorescence

We used ready-made diode lasers from Laserglow as light sources, one at 473 nm and one at 532 nm. These were powerful enough to burn the sample under magnification after several seconds. To prevent this, we introduced a polarizer into the beam path and set the power to a lower, steady-state value that would not cause damage over several hours. This was necessary, as our scans would routinely take from 2 to 6 hours in duration, due to low signals characteristic of Raman spectra. These parameters were used so that all spectra were normalized for exposure time, input power, and the quantum efficiency of the SBIG CCD.

Before we can compare the enhanced Raman spectra, there are two other factors that influence the data that we need to discuss. The first is the excitation-frequency-to-the-fourth-power dependence of the Raman signal. This needs to be normalized for before comparing Raman signal levels at different frequencies. The second factor of importance is fluorescence. Generally, higher frequencies (energies) cause more fluorescence than lower ones; so shorter wavelengths are more likely to have a larger fluorescence background under the Raman spectra than longer wavelengths. In our case, it means that a background rising towards larger delta-wavenumbers is expected for the 473 nm excitation, but not as significant for the 532 nm excitation.

3. RESULTS

3.1 Analysis of Enhancement

In both whole blood spectra, we see large peaks on resonance, and smaller peaks off resonance. Here we use a simplified analysis to estimate the peak enhancement due to resonance Raman effects. To first order, we can assume the background follows a straight line. For our whole blood spectra this is an acceptable condition, as our peaks are relatively narrow. We can establish a background level by interpolating a background point at the peak maximum using a linear equation. We can further correct for the well known $\frac{1}{\lambda^4}$ dependency to extract a wavelength-independant resonance enhancement ratio. This works for defining the enhancement ratio when we can pick a defined peak out of both spectra. When we cannot find the off-resonance peak, we have to assume that it is smaller than the local variance exhibited by the spectra. We can then take the local noise as a limit on the peak height, so our calculations give us a lower limit on the resonance enhancement ratio.

We calculated the relative enhancements for our whole blood spectra, pictured in Fig. 2, and plotted the results by graphing the enhancement ratio grouped by symmetry, and versus wavelength shift. These can be found in Fig. 2. We note a fairly well established correlation by wavelength shift, indicating the lower energy, lower change in wavenumber modes were in general less enhanced than the higher energy, higher change in wavenumber modes. We also note that the specific symmetry groups did not show a definitive trend that could not be explained by the above correlation. This indicates that our resonance enhancement spectra, like our absorbance spectra, is mostly dominated by longer-range vibrational modes.

3.2 Resonant vessels

In this section we show that resonance is observed in the Raman signal from ancient vessel fragments, which strongly suggests that a significant portion of the hemoglobin molecule is still intact. The Raman spectral features have changed, however, showing that the molecule has undergone some modification. Fig. 3 contains Raman spectra of a particular region of what appears to be blood vessel remains of a brachylophosaurus. The on-resonance spectrum is somewhat similar to that of Fig. 2, although clearly modified.

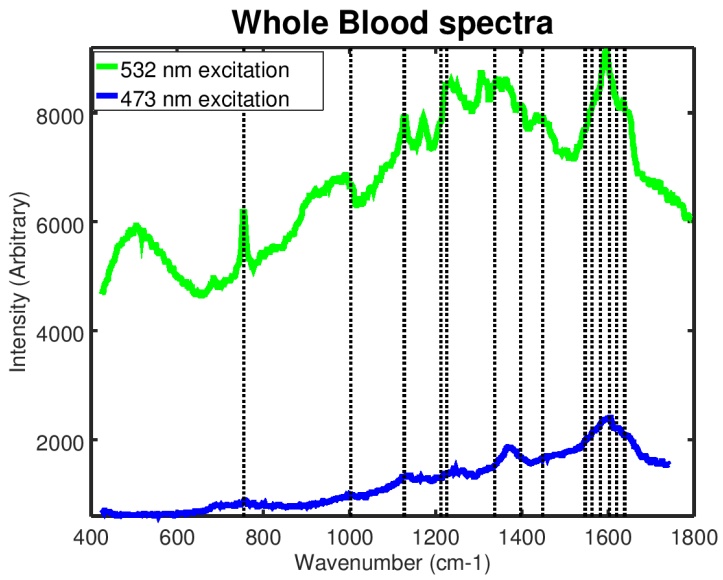

(a)

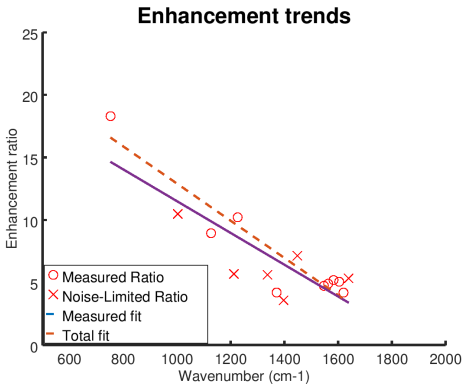

(b)

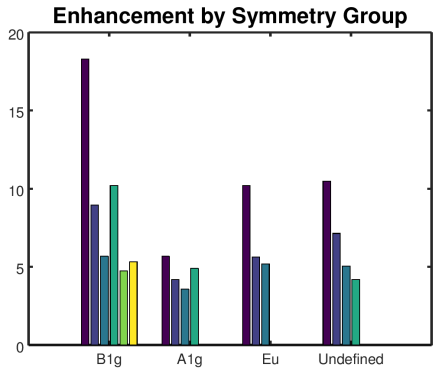

(c)

Figure 2 The ratio of resonance-enhanced, 532 nm excitation raman peaks, to non-resonance enhanced, 473 excitation peaks, plotted by (a) wavenumber shift and (b) symmetry group. We note that the ratios are well correlated by energy, but not by symmetry.

In general, there is significantly few defined Raman peaks, but much greater intensity compared to whole blood (Fig. 2). This can likely be attributed to far less pristine hemoglobin or hemoglobin derivatives than in whole blood, as well as other optical signals. We see significant spectral features that indicate the presence of a hemoglobin derivative. It also has much higher signal levels than the off-resonance spectrum with 473 nm excitation, indicating that the parts of the hemoglobin molecule that are absorbing near 532 nm are still intact. The 473 nm excitation spectra is far more driven by fluorescent background, perhaps due to collagen's well known fluorescent activity.[53–56] We note that the wide variety of possible macromolecules in these vessels means that other possibilities besides collagen may be responsible for the fluorescence and broad Raman peaks.

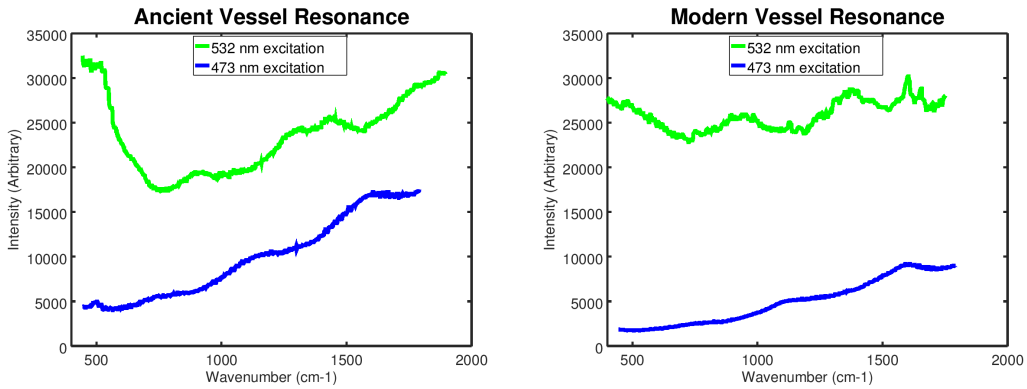

(a) **(b)**

Figure 3 Micro-Raman spectra of a) ancient vessel fragments and b) modern vessel samples using excitation energies of 473 nm (off-resonance) and 532 nm (on resonance for hemoglobin). The spectra have been corrected for power, but the background has not been subtracted. Note the gains from the resonance are selectively applied to the hemoglobin spectra.

Since we have calculated our enhancements from a reference sample, it is prudent to indicate how many of our peaks would be expected to be visible above the noise in the 473 spectra. This, of course, assumes that the enhancement ratio is constant across samples, as it should be for the same molecules. It also assumes that the concentration of hemoglobin or hemoglobin derivatives is not significantly changing during the time we change the excitation laser, as it should since we are operating below the damage threshold. For our calculations, we used our deoxygenated modern samples, prepared as described in Section 2.1.2. We found that the estimated peak heights for most peaks in the 473 nm, non-resonant, hemoglobin-related Raman spectra, calculated from whole blood measurements, should not rise above the noise level measured in our spectra. However, the calculations indicate that a few peaks may possibly break through the local noise. We see little evidence of these peaks in the non-resonant spectra, suggesting that they were subsumed by the whole tissue Raman spectra or the fluorescent background. This further emphasizes the need to use resonance measurements to help select the Raman signals from the desired macromolecules. As we saw in the 532 nm excitation data, resonance Raman is enhanced over background, showing both evidence for the existence of our target molecule, hemoglobin, in the sample, and also allowing us to study the specific modes in this hemoglobin derivative.

4. CONCLUSION

We have shown that the use of resonance Raman in complex biological materials provides a double-selectivity for the molecules of interest, which can simplify the analysis so that conclusions can be made about the presence of certain absorbing structures in the system. This is made even more useful when the sample contains many chemical species that are as of yet not positively identified. Comparison between on and off resonance spectra is useful. In our case, we demonstrate that enough of the hemoglobin molecule remains in soft tissue recovered from demineralized bone of ancient fossils that absorption still takes place and the enhanced Raman spectra

indicates some similar features, and some modifications to the molecule. The use of resonance Raman and the evidence given for hemoglobin-like resonance gives yet more evidence for an ancient origin of these vessels, and of the hemoglobin derived compounds within them. We look forward to applying this technique with other biological markers, especially if we can use these biological markers to indicate different environmental factors. Further analysis of the Raman spectral peaks and their meanings in scenarios described here will appear in a later publication.

ACKNOWLEDGMENTS

We thank Wenxia Zheng and Mary Schweitzer for samples and useful discussions.

REFERENCES

[1] Faghihzadeh, F., Anaya, N., Hadjeres, H., Boving, T., and Oyanedel-Craver, V., "Pulse uv light effect on microbial biomolecules and organic pollutants degradation in aqueous solutions," *Chemosphere* **216**, 677 – 683 (2019).

[2] Shigemitsu, H., Fujisaku, T., Onogi, S., Yoshii, T., Ikeda, M., and Hamachi, I., "Preparation of supramolecular hydrogel-enzyme hybrids exhibiting biomolecule-responsive gel degradation," *Nature Protocols* **11**, 1744–1756 (09 2016). Copyright - Copyright Nature Publishing Group Sep 2016; Last updated - 2016-08-31.

[3] Liu, H., "The effects of surface and biomolecules on magnesium degradation and mesenchymal stem cell adhesion," *Journal of Biomedical Materials Research Part A* **99A**(2), 249–260 (2011).

[4] Zhang, X., Li, X., Zhang, Q., Yang, J., and Deng, N., "Efficient photodegradation of 4,4'-(propane-2,2-diyl)diphenol over biomolecule modified titanium dioxide under visible light irradiation," *Catalysis Communications* **16**(1), 7 – 10 (2011).

[5] Lindgren, J., Uvdal, P., Engdahl, A., Lee, A. H., Alwmark, C., Bergquist, K.-E., Nilsson, E., Ekström, P., Rasmussen, M., Douglas, D. A., et al., "Microspectroscopic evidence of cretaceous bone proteins," *PLoS One* **6**(4), e19445 (2011).

[6] Cadena, E. and Schweitzer, M., "Preservation of blood vessels and osteocytes in a pelomedusoid turtle from the paleocene of colombia," *J Herpetol* **48**(3), 125–129 (2014).

[7] Lindgren, J., Kuriyama, T., Madsen, H., Sjövall, P., Zheng, W., Uvdal, P., Engdahl, A., Moyer, A. E., Gren, J. A., Kamezaki, N., Ueno, S., and Schweitzer, M. H., "Biochemistry and adaptive colouration of an exceptionally preserved juvenile fossil sea turtle," *Scientific Reports (Nature Publisher Group)* **7**, 1–13 (10 2017). Copyright - © 2017. This work is published under http://creativecommons.org/licenses/by/4.0/ (the "License"). Notwithstanding the ProQuest Terms and Conditions, you may use this content in accordance with the terms of the License; Last updated - 2018-10-17.

[8] Cleland, T. P., Schroeter, E. R., Zamdborg, L., Zheng, W., Lee, J. E., Tran, J. C., Bern, M., Duncan, M. B., Lebleu, V. S., Ahlf, D. R., Thomas, P. M., Kalluri, R., Kelleher, N. L., and Schweitzer, M. H., "Mass spectrometry and antibody-based characterization of blood vessels from brachylophosaurus canadensis," *Journal of Proteome Research* **14**(12), 5252–5262 (2015). PMID: 26595531.

[9] Pan, Y., Zheng, W., Moyer, A. E., O'Connor, J. K., Wang, M., Zheng, X., Wang, X., Schroeter, E. R., Zhou, Z., and Schweitzer, M. H., "Molecular evidence of keratin and melanosomes in feathers of the early cretaceous bird eoconfuciusornis," *Proceedings of the National Academy of Sciences* **113**(49), E7900–E7907 (2016).

[10] Schweitzer, M. H., "Soft tissue preservation in terrestrial mesozoic vertebrates," *Annual Review of Earth and Planetary Sciences* **39**(1), 187–216 (2011).

[11] Schweitzer, M. H., Wittmeyer, J. L., and Horner, J. R., "Soft tissue and cellular preservation in vertebrate skeletal elements from the cretaceous to the present," *Proceedings of the Royal Society B: Biological Sciences* **274**(1607), 183 (2007).

[12] Schweitzer, M. H., Zheng, W., Organ, C. L., Avci, R., Suo, Z., Freimark, L. M., Lebleu, V. S., Duncan, M. B., Heiden, M. G. V., Neveu, J. M., Lane, W. S., Cottrell, J. S., Horner, J. R., Cantley, L. C., Kalluri, R., and Asara, J. M., "Biomolecular characterization and protein sequences of the campanian hadrosaur b. canadensis," *Science* **324**(5927), 626–631 (2009).

[13] Asara, J. M., Schweitzer, M. H., Freimark, L. M., Phillips, M., and Cantley, L. C., "Protein sequences from mastodon and tyrannosaurus rex revealed by mass spectrometry," *Science* **316**(5822), 280–285 (2007).

[14] Schroeter, E. R., DeHart, C. J., Schweitzer, M. H., Thomas, P. M., and Kelleher, N. L., "Bone protein "extractomics": comparing the efficiency of bone protein extractions of *Gallus gallus* in tandem mass spectrometry, with an eye towards paleoproteomics," *PeerJ* **4**, e2603 (Oct. 2016).

[15] Schweitzer, M. H., Zheng, W., Cleland, T. P., and Bern, M., "Molecular analyses of dinosaur osteocytes support the presence of endogenous molecules," *Bone* **52**, 414–423 (Jan 2013).

[16] Schroeter, E. R., DeHart, C. J., Cleland, T. P., Zheng, W., Thomas, P. M., Kelleher, N. L., Bern, M., and Schweitzer, M. H., "Expansion for the brachylophosaurus canadensis collagen i sequence and additional evidence of the preservation of cretaceous protein," *Journal of Proteome Research* **16**(2), 920–932 (2017). PMID: 28111950.

[17] Schweitzer, M. H., Marshall, M., Carron, K., Bohle, D. S., Busse, S. C., Arnold, E. V., Barnard, D., Horner, J., and Starkey, J. R., "Heme compounds in dinosaur trabecular bone," *Proceedings of the National Academy of Sciences* **94**(12), 6291–6296 (1997).

[18] Raman, C. V. and Krishnan, K. S., "A new type of secondary radiation," *Nature* **121**(3048), 501 (1928).

[19] Anderson, A., [*The Raman effect: applications*], vol. 2, M. Dekker (1973).

[20] Jahncke, C. L., Paesler, M. A., and Hallen, H. D., "Raman imaging with nearfield scanning optical microscopy," *Applied Physics Letters* **67**(17), 2483–2485 (1995).

[21] Hallen, H. D., "Nano-raman spectroscopy: Surface plasmon emission, field gradients, and fundamentally near field propagation effects," *Nanobiotechnology* **3**, 197–202 (12 2007). Copyright - Humana Press Inc. 2009; Last updated - 2011-06-01.

[22] Ayars, E. J. and Hallen, H. D., "Surface enhancement in near-field raman spectroscopy," *Applied Physics Letters* **76**(26), 3911–3913 (2000).

[23] Grasselli, J. G., Snavely, M. K., and Bulkin, B. J., [*Chemical applications of Raman spectroscopy*], John Wiley & Sons Inc (1981).

[24] Long, D. A., [*The Raman Effect*], Wiley (2002).

[25] Ayars, E. J., Hallen, H. D., and Jahncke, C. L., "Electric field gradient effects in raman spectroscopy," *Phys. Rev. Lett.* **85**, 4180–4183 (Nov 2000).

[26] Balsiger, F. and Philbrick, C. R., "Comparison of lidar water vapor measurements using raman scatter at 266 nm and 532 nm," in [*Application of Lidar to Current Atmospheric Topics*], **2833**, 231–241, International Society for Optics and Photonics (1996).

[27] Willitsford, A., Chadwick, C. T., Hallen, H., Kurtz, S., and Philbrick, C. R., "Resonance enhanced raman scatter in liquid benzene at vapor-phase absorption peaks," *Optics Express* **21**(22), 26150–26161 (2013).

[28] Li, L., Fang Lim, S., Puretzky, A. A., Riehn, R., and Hallen, H. D., "Near-field enhanced ultraviolet resonance raman spectroscopy using aluminum bow-tie nano-antenna," *Applied Physics Letters* **101**(11), 113116 (2012).

[29] Kaye, T. G., Gaugler, G., and Sawlowicz, Z., "Dinosaurian soft tissues interpreted as bacterial biofilms," *PLoS One* **3**(7), e2808 (2008).

[30] Schweitzer, M. H., Moyer, A. E., and Zheng, W., "Testing the hypothesis of biofilm as a source for soft tissue and cell-like structures preserved in dinosaur bone," *PloS one* **11**(2), e0150238 (2016).

[31] Ahmad, S. R. and Foster, V. G., "Pre-resonance raman scattering in nitrobenzene vapour," *Journal of Raman Spectroscopy* **31**(11), 1023–1028 (2000).

[32] Asher, S. A., "Uv resonance raman spectroscopy for analytical, physical, and biophysical chemistry. part 1," *Analytical Chemistry* **65**(2), 59A–66A (1993).

[33] Clark, R. J. and Dines, T. J., "Resonance raman spectroscopy, and its application to inorganic chemistry. new analytical methods (27)," *Angewandte Chemie International Edition in English* **25**(2), 131–158 (1986).

[34] Efremov, E. V., Ariese, F., and Gooijer, C., "Achievements in resonance raman spectroscopy: Review of a technique with a distinct analytical chemistry potential," *Analytica Chimica Acta* **606**(2), 119 – 134 (2008).

[35] Lee, S., "Placzektype polarizability tensors for raman and resonance raman scattering," *The Journal of Chemical Physics* **78**(2), 723–734 (1983).

[36] Li, L., Lim, S. F., Puretzky, A., Riehn, R., and Hallen, H. D., "Dna methylation detection using resonance and nanobowtie-antenna-enhanced raman spectroscopy," *Biophysical Journal* **114**(11), 2498 – 2506 (2018).

[37] Hallen, H. D., Willitsford, A., Weeks, R., and Philbrick, C. R., "Uv resonance raman signatures of phonon-allowed absorptions and phonon-driven bubble formation," in [*Ultrafast Nonlinear Imaging and Spectroscopy III*], **9584**, 95840P, International Society for Optics and Photonics (2015).

[38] Willitsford, A., Chadwick, C. T., Hallen, H., Kurtz, S., and Philbrick, C. R., "Resonance enhanced raman scatter in liquid benzene at vapor-phase absorption peaks," *Opt. Express* **21**, 26150–26161 (Nov 2013).

[39] Long, B., Zheng, W., Schweitzer, M., and Hallen, H., "Resonance raman imagery of semi-fossilized soft tissues," in [*Ultrafast Nonlinear Imaging and Spectroscopy VI*], **10753**, 1075310, International Society for Optics and Photonics (2018).

[40] Schweitzer, M. H., Zheng, W., Cleland, T. P., Goodwin, M. B., Boatman, E., Theil, E., Marcus, M. A., and Fakra, S. C., "A role for iron and oxygen chemistry in preserving soft tissues, cells and molecules from deep time," *Proceedings of the Royal Society B: Biological Sciences* **281**(1775) (2014).

[41] Buettner, G. R. and Jurkiewicz, B. A., "Catalytic metals, ascorbate and free radicals: combinations to avoid," *Radiation research* **145**(5), 532–541 (1996).

[42] Perutz, M. F., "Regulation of oxygen affinity of hemoglobin: Influence of structure of the globin on the heme iron," *Annual Review of Biochemistry* **48**(1), 327–386 (1979). PMID: 382987.

[43] Ryter, S. W. and Tyrrell, R. M., "The heme synthesis and degradation pathways: role in oxidant sensitivity: Heme oxygenase has both pro- and antioxidant properties," *Free Radical Biology and Medicine* **28**(2), 289 – 309 (2000).

[44] Berg, J., Tymoczko, J., Stryer, L., and Stryer, L., "Biochemistry, ed 5th," (2002).

[45] Nitzan, M., Romem, A., and Koppel, R., "Pulse oximetry: fundamentals and technology update," *Medical Devices (Auckland, NZ)* **7**, 231 (2014).

[46] Chu, G. C., Katakura, K., Zhang, X., Yoshida, T., and Ikeda-Saito, M., "Heme degradation as catalyzed by a recombinant bacterial heme oxygenase (hmu o) from corynebacterium diphtheriae," *Journal of Biological Chemistry* **274**(30), 21319–21325 (1999).

[47] Ramzannezhad, A., Gill, P., and Bahari, A., "Fabrication of magnetic nanorods and their applications in medicine," *BioNanoMaterials* **18**(3-4) (2017).

[48] Snow, C. L., Martineau, L. N., Hilton, R. J., Brown, S., Farrer, J., Boerio-Goates, J., Woodfield, B. F., and Watt, R. K., "Ferritin iron mineralization proceeds by different mechanisms in mops and imidazole buffers," *Journal of Inorganic Biochemistry* **105**(7), 972 – 977 (2011).

[49] Singh, A., Chowdhury, D. R., and Paul, A., "A kinetic study of ferrocenium cation decomposition utilizing an integrated electrochemical methodology composed of cyclic voltammetry and amperometry," *Analyst* **139**, 5747–5754 (2014).

[50] Herrera, F. V., Grez, P., Schrebler, R., Ballesteros, L. A., Muñoz, E., Córdova, R., Altamirano, H., and Dalchiele, E. A., "Preparation and photoelectrochemical characterization of porphyrin-sensitized α-fe2o3 thin films," *Journal of The Electrochemical Society* **157**(5), D302–D308 (2010).

[51] Panwar, V., Kumar, P., Bansal, A., Ray, S. S., and Jain, S. L., "Pegylated magnetic nanoparticles (peg@ fe3o4) as cost effective alternative for oxidative cyanation of tertiary amines via ch activation," *Applied Catalysis A: General* **498**, 25–31 (2015).

[52] Loures, C. C., Alcântara, M. A., Izário Filho, H. J., Teixeira, A., Silva, F. T., Paiva, T. C., and Samanamud, G. R., "Advanced oxidative degradation processes: fundamentals and applications," *International Review of Chemical Engineering* **5**(2), 102–120 (2013).

[53] Zou, L., Koslakiewicz, R. J., Mahmoud, M., Fahs, M., Liu, R., and Lo, J. F., "Three-dimensional printed miniaturized spectral system for collagen fluorescence lifetime measurements," *Journal of biomedical optics* **21**(7), 075001 (2016).

[54] Sell, D. R., Nemet, I., and Monnier, V. M., "Partial characterization of the molecular nature of collagen-linked fluorescence: Role of diabetes and end-stage renal disease," *Archives of Biochemistry and Biophysics* **493**(2), 192 – 206 (2010).

[55] Babu, P. V. A., Sabitha, K. E., Srinivasan, P., and Shyamaladevi, C. S., "Green tea attenuates diabetes induced maillard-type fluorescence and collagen cross-linking in the heart of streptozotocin diabetic rats," *Pharmacological Research* **55**(5), 433 – 440 (2007).

[56] Menter, J. M., "Temperature dependence of collagen fluorescence," *Photochem. Photobiol. Sci.* **5**, 403–410 (2006).